Published in final edited form as:
Virology. 2009 January 20; 383(2): 237–247. doi:10.1016/j.virol.2008.10.029.

Requirements for Cell Rounding and Surface Protein Down-Regulation by Ebola Virus Glycoprotein

Joseph R. Francica, **Meghan K. Matukonis**, and **Paul Bates***
Department of Microbiology, University of Pennsylvania School of Medicine, 225 Johnson Pavilion, 3610 Hamilton Walk, Philadelphia, PA 19104-6076

Abstract

Ebola virus causes an acute hemorrhagic fever that is associated with high morbidity and mortality. The viral glycoprotein is thought to contribute to pathogenesis, though precise mechanisms are unknown. Cellular pathogenesis can be modeled *in vitro* by expression of the Ebola viral glycoprotein (GP) in cells, which causes dramatic morphological changes, including cell rounding and surface protein down-regulation. These effects are known to be dependent on the presence of a highly glycosylated region of the glycoprotein, the mucin domain. Here we show that the mucin domain from the highly pathogenic Zaire subtype of Ebola virus is sufficient to cause characteristic cytopathology when expressed in the context of a foreign glycoprotein. Similarly to full length Ebola GP, expression of the mucin domain causes rounding, detachment from the extracellular matrix, and the down-regulation of cell surface levels of β1 integrin and major histocompatibility complex class 1. These effects were not seen when the mucin domain was expressed in the context of a glycophosphatidylinositol-anchored isoform of the foreign glycoprotein. In contrast to earlier analysis of full length Ebola glycoproteins, chimeras carrying the mucin domains from the Zaire and Reston strains appear to cause similar levels of down-modulation and cell detachment. Cytopathology associated with Ebola glycoprotein expression does not occur when GP expression is restricted to the endoplasmic reticulum. In contrast to a previously published report, our results demonstrate that GP-induced surface protein down-regulation is not mediated through a dynamin-dependent pathway. Overall, these results support a model in which the mucin domain of Ebola GP acts at the cell surface to induce protein down modulation and cytopathic effects.

Introduction

Ebola virus is a member of the family *Filoviridae*, and causes a severe hemorrhagic fever in humans and non-human primates (Sanchez et al., 2001). In cell culture, Ebola virus infection causes pathogenic effects that result in destruction the monolayer (Alazard-Dany et al., 2006; Barrientos and Rollin, 2006). The specific determinants of viral pathogenicity *in vivo* are still unknown; however, the viral glycoproteins are thought to play a large role in cellular pathogenesis (Chan, Ma, and Goldsmith, 2000; Volchkov et al., 2001; Yang et al., 2000). The Ebola virus encodes two forms of its glycoprotein, a dimeric secreted form (sGP) (Volchkova et al., 1998) and a trimeric membrane-spanning form, GP, which originates from RNA editing of the glycoprotein ORF (Sanchez et al., 1996). No cellular toxcicity has been associated with

*Corresponding author: Department of Microbiology, University of Pennsylvania School of Medicine, 225 Johnson Pavilion, 3610 Hamilton Walk, Philadelphia, PA 19104-6076, Telephone: (215) 573-3509, FAX: (215) 573-9068, e-mail: pbates@mail.med.upenn.edu.

sGP; however, because it is the predominant form that is transcribed and translated, it is thought that the balance between sGP and GP may be necessary to control the cytopathic effects attributed to GP (Volchkov et al., 2001; Yang et al., 2000). When expressed *in vitro* and *in vivo*, GP causes cell rounding, detachment, and down-regulation of many surface proteins (Simmons et al., 2002; Takada et al., 2000; Yang et al., 2000). Among the surface proteins down-modulated by GP are β1 integrin (CD 29), α5 integrin, αV integrin, and major histocompatibility complex class 1 (MHC1) in 293T cells (Simmons et al., 2002). However, the exact profile of protein down-regulation seems to differ by cell type. In primary human cardiac microvascular endothelial cells GP expression, and the resultant loss of adhesion, induces anoikis (Ray et al., 2004), whereas cell lines, such as human 293T, remain viable after cellular detachment (Simmons et al., 2002).

Analysis of Ebola GP deletion mutants demonstrated that these morphological changes, along with the down-regulation of surface proteins, are dependent on a highly O- and N-glycosylated domain within GP, termed the mucin domain (Simmons et al., 2002; Sullivan et al., 2005; Takada et al., 2000; Yang et al., 2000). The mucin domain is approximately 150 amino acids in length and is a conserved feature of filoviruses, though the primary sequence is highly variable among subtypes and strains. The domain is thought to have little secondary or tertiary structure because of its high level of glycosylation. Biochemical analysis has shown that after cleavage of the glycoprotein precursor by furin (Volchkov et al., 1998) into GP_1 (receptor-recognizing) and GP_2 (membrane-spanning) fragments, the N-terminus of GP_1 remains associated with GP_2, leaving the mucin domain exposed at the C-terminus of GP_1 (Sanchez et al., 1998). The mucin domain is not necessary for GP surface expression or formation of infectious pseudotyped virions (Manicassamy et al., 2005; Medina et al., 2003; Yang et al., 2000). There is no single region of the domain that contributes disproportionately to the rounding phenotype, indicating that the phenotype may be dependent on the overall size of the domain or level of its glycosylation (Simmons et al., 2002).

Other viruses, such as the Bunyavirus, Crimean Congo Hemorrhagic Fever Virus (CCHV) and the polydnavirus, *Microplitis demolitor* bracovirus (MdBV), encode proteins with mucin-like domains. While no rounding or other cytopathology has been reported for the CCHV mucin-like protein, the MdBV protein Glc1.8 causes rounding when transfected into insect cells in a manner dependent on membrane association (Beck and Strand, 2005). In addition, the cellular mucin protein MUC1 (episialin) has been shown to play a direct role in the disruption of attachment factors such as β1 integrin when expressed in melanoma and epithelial cell lines (Wesseling et al., 1995). MUC1 is known to be highly and aberrantly expressed in many adenocarcinomas and its expression correlates with increased metastasis and poor prognosis (McGuckin et al., 1995; Osako et al., 1993; Yamashita et al., 1993). MUC1 is thought to interfere with adhesion through steric hindrance of necessary adhesion molecules (Wesseling et al., 1995). In addition, it has been shown that the size of the glycosylated region of MUC1 positively contributes to its ability to interfere with E-cadherin-based cell-cell interactions (Wesseling, van der Valk, and Hilkens, 1996). This data agrees with our previously-published study, which correlated the rounding phenotype to the size of the Ebola Zaire GP mucin domain (Simmons et al., 2002).

Although it has been well documented that the presence of the mucin domain is necessary for GP-mediated cytopathology, it has yet to be shown that the mucin domain is fully sufficient to induce the effects discussed above. One report found that murine leukemia virus amphotropic envelope containing the mucin domain caused an increase in floating cells in culture (Yang et al., 2000). Here we analyzed the requirements for Ebola GP-mediated cytopathology. We show that the mucin domains from both the Zaire and Reston subtypes of the Ebola virus are sufficient to cause morphological alterations characteristic of GP expression by placing these domains in the context of a heterologous, monomeric glycoprotein. Using isoforms of this heterologous

protein, we further demonstrate that a membrane-bound form induces cytopathology, whereas a lipid-(GPI) anchored isoform does not. Moreover, little is known about the mechanism of GP-induced cytopathology. Here we show that cytopathology associated with the expression of GP does not occur when GP is restricted to the endoplasmic reticulum (ER). It has also been reported that the down-regulation of surface proteins by Ebola GP is likely mediated through a dynamin-dependent pathway (Sullivan et al., 2005). However, data reported here support the alternative hypothesis that this process occurs independently of dynamin.

Results

Characterization of Tva-mucin chimeric constructs

To investigate whether the mucin domain of Ebola GP is sufficient to cause cell rounding and protein down-regulation, we created constructs in which the mucin domain was placed into the heterologous, small monomeric glycoprotein, Tva. Tva is an avian glycoprotein and is the cellular receptor for subgroup A avian sarcoma and leukosis virus (ASLV) (Bates, Young, and Varmus, 1993). The quail Tva locus also produces a naturally-occurring splice variant that associates with membranes through a GPI anchor instead of a transmembrane domain (P. Bates, unpublished data), termed here, GPI Tva. The mucin domain from the Zaire subtype of Ebola GP was cloned into vectors expressing both isoforms of Tva to create expression plasmids for the proteins designated here as Tva-muc and GPI Tva-muc (Fig. 1A). Analysis of lysates produced from 293T cells transfected with these constructs demonstrated processing differences among the proteins (Fig. 1B). The multiple bands within each lane represent glycosylation variants of the proteins while differences between lanes reflect the transmembrane- verses GPI- anchored forms and the added mucin domain. To investigate the cellular localization of these proteins, immunofluorescence was performed on HeLa cells transfected with each construct (Fig. 1C). Staining with a polyclonal antibody to a Tva peptide showed both plasma membrane and cytoplasmic staining of each of the proteins. Expression of the transmembrane-bound isoforms, Tva and Tva-muc exhibits a punctuate or vesicular cytoplasmic staining, whereas GPI Tva and GPI Tva-muc show more of a reticular cytoplasmic staining pattern. Addition of the mucin domain to either of the Tva isoforms did not cause any significant change in the observed staining patterns (Fig. 1C).

GP mucin domain is sufficient to cause GP-characteristic cytopathology

To address whether the expression of the chimeric mucin domain proteins could induce similar morphological changes to those seen upon expression of Ebola GP, each of the Tva constructs described above was mixed with an eGFP encoding vector and used to transfect 293T cells. 24 hours after transfection, fluorescence microscopy was performed to visualize transfected cells (Fig. 1D). While transfection of Tva or GPI Tva did not induce any change in cell morphology, cells transfected with Tva-muc were rounded and many had lost their ability to adhere to the extracellular matrix. In contrast, the transfection of GPI Tva-muc had no effect on cell morphology. To quantify the mucin domain-induced loss of adhesion to the extracellular matrix, 293T cells were co-transfected with the Tva constructs and an eCFP-encoding vector. Floating and adherent cells were removed 24 hours post-transfection; only transfected (CFP positive) cells were counted. Expression of Tva-muc caused cell detachment that was over ten-fold higher than background levels (Fig. 1E). Transfection with Tva, GPI Tva, or GPI Tva-muc did not result in cellular detachment significantly above background levels.

To further characterize the effects of the Ebola mucin domain on cellular physiology, we used flow cytometry to measure surface levels of β1 integrin and MHC1 in transfected cells. Both of these proteins are known to be down-regulated from the surface of cells expressing high levels of Ebola GP (Simmons et al., 2002; Takada et al., 2000). Cells that were transfected with Tva showed no change in levels of β1 integrin or MHC1 after 24 hours; however, cells

transfected with Tva-muc showed a roughly one log decrease in fluorescence of both proteins (Fig. 2). Close inspection of the FACS plots reveals that cells with low expression of Tva-muc have intact levels of β1 integrin and MHC1; however, there seems to be a threshold of Tva-muc expression, above which β1 integrin and MHC1 levels drop precipitously. By contrast, this threshold effect is not seen with GPI Tva-muc. The GPI Tva-muc sample has expression levels of the chimeric protein that would be predicted to cause down-regulation of β1 integrin and MHC1, yet this is not observed. From these results we conclude that the mucin domain of Ebola GP, when expressed within the context of a transmembrane-bound form of Tva, is sufficient to cause cytopathology characteristic of full-length GP expression.

Reston is considered to be the least pathogenic subtype of Ebola, while Zaire is the most pathogenic (Fisher-Hoch et al., 1992). Previous analysis of the glycoproteins from these two Ebola subtypes suggests that while both glycoproteins cause cytopathic effects, Zaire GP appears to cause greater levels of cell rounding and surface protein down modulation (Simmons et al., 2002). To address whether the isolated mucin domains of different subtypes of Ebola virus differ in their ability to cause cytopathology, we directly compared chimeric proteins carrying the mucin regions from Ebola Zaire to Ebola Reston. The mucin domain of Ebola Reston was expressed within the transmembrane-bound form of Tva. Analysis by flow cytometry revealed that 293T cells transfected with chimeric Tva carrying the mucin domain from Reston or Zaire subtypes demonstrated similar levels of surface expression and equal reduction of β1 integrin and MHC1 surface staining after 24 hours (data not shown). In addition, chimeras carrying the Reston mucin domain induced significant cell rounding similar to that observed with the Zaire constructs. Overall, these results, when compared to previous analyses, suggest that the ability of the mucin domains to induce rounding may be modulated by the context in which they are presented.

Characterization of GP-kk

To address whether GP could exert its effects from the endoplasmic reticulum or if transport to the cell surface is required, we created a version of the Ebola GP with an ER retention signal, KKMP, appended to the cytoplasmic tail of the protein (GP-kk). Analysis of lysates made from 293T cells transfected with GP and GP-kk demonstrated that the constructs were expressed to a similar level (Fig. 3A). To characterize the glycosylation state of GP-kk, lysates from GP or GP-kk transfected cells were incubated with PNGase F, which removes all N-linked glycans, and Endo H_f, which removes high-mannose glycans, characteristic of proteins that have not matured through the Golgi (Fig. 3B). When incubated with Endo H_f, the majority of GP-kk protein co-migrates with PNGase F digested protein on SDS-PAGE. This Endo H_f sensitivity suggests that GP-kk is not transported to the Golgi and remains in the ER. By comparison, the majority of GP is resistant to Endo H_f digestion, as would be expected of protein that has matured through the Golgi.

GP cellular localization

To further examine the localization of GP-kk, immunofluorescence was performed on HeLa cells transfected with GP and GP-kk (Fig. 3C). Permeabilized and non-permeabilized cells were stained with a monoclonal antibody to Ebola GP and co-stained with an antibody to GM-130, a *cis*-Golgi localized scaffold protein, to test the integrity of the plasma membrane during staining (Fig. 3C, top and middle panels). GP-transfected cells displayed intense plasma membrane staining in both permeabilized and non-permeabilized cells. Some internal vesicular staining was noted for GP, however this showed no significant colocalization with GM-130 (Fig. 3C, middle panels). By contrast, only very few non-permeabilized cells transfected with GP-kk showed any surface staining (data not shown). For the majority of GP-kk expressing cells, GP staining could only be seen upon permeablization (Fig. 3C, bottom panels). Staining of these cells revealed a cytoplasmic, reticular pattern. GP-kk appeared to co-localize with

staining of the ER-resident protein, calnexin, but did not demonstrate detectable colocalization with GM-130 (data not shown). Thus, we conclude that GP-kk is actively retained in the ER through its retention signal.

GP-kk does not cause cytopathology

We then asked whether retaining Ebola GP in the ER had any effect on cell rounding and protein down-regulation. 293T cells were transfected with GP, GP-kk, or the empty vector and co-transfected with eGFP as above. 24 hours after transfection, microscopy was performed using a GFP filter so that only transfected cells were visualized (Fig. 3D). Cells transfected with the vector were flat and adherent, whereas GP transfected cells were rounded and floating. Cells that had been transfected with GP-kk were morphologically indistinguishable from the vector control. To quantitate this result, floating and adherent cells in culture dishes were counted 24 hours after co-transfection of the GP constructs with an eCFP-encoding vector (Fig. 3E). The addition of the ER retention signal to GP resulted in a reduction the number of floating cells by approximately 98%, to background levels. 293T cells transfected with GP or GP-kk were stained with antibodies to Ebola GP and β1 integrin or MHC1 and analyzed by flow cytometry. Whereas GP strongly down-regulated β1 integrin and MHC1, GP-kk did not (Fig. 4). Flow cytometric analysis of GP-kk transfected cells, surfaced stained for Ebola GP, reveals that a small percentage of transfected cells express GP-kk on the surface, despite the ER retention signal (Fig. 4). This observation is supported by immunofluorescence studies, where some surface-stained cells are observed, and also endoglycosidase assay data (Fig. 3B), in which a small amount of Endo Hf-resistant protein in the GP-kk sample is visible. Interestingly, in the small amount of cells that show some surface staining for GP-kk, levels of β1 integrin and MHC1 do not appear altered. It should also be noted that GP-transfected cells show down-regulation of GP from the surface resulting in comma-shaped FACS plots (Fig. 4A, B). However, this comma-shaped profile was not observed with the Tva constructs (Fig. 2A, B). These data allow us to conclude that the Ebola GP does not cause morphological changes and protein down-regulation when retained in the ER.

Surface protein down-regulation is not mediated through a dynamin-dependent pathway

To address whether surface protein down-regulation was affected by the expression of a dominant-negative version of dynamin as previously reported (Sullivan et al., 2005), we employed a construct expressing human dynamin I with a K44A mutation (Dyn K44A). This mutation is known to disrupt coated vesicle formation and trafficking by exerting a dominant negative effect on dynamin's role in vesicle formation (Damke et al., 1994). Analysis of lysates made from 293T cells transfected with Dyn K44A demonstrated that the construct was expressed and that the dynamin I antibody specifically recognized the transfected dynamin I protein, not endogenous dynamin II (Fig. 5A). To examine the ability of Dyn K44A to block vesicle trafficking, a transferrin uptake assay was performed. As shown in Fig. 5B, labeled transferrin bound the surface of HeLa cells at 4 °C. When incubated at 37 °C for 15 min., cells internalized the transferrin; however, transferrin remained at the surface of cells transfected with Dyn K44A. This effect was also seen after incubation for 30 min.; after 60 min the transferrin was mostly degraded (data not shown). Thus, our Dyn K44A behaves as a functional dominant negative of dynamin-dependent pathways.

We then addressed whether the expression of Dyn K44A would alter the level of surface protein down-regulation in GP-transfected cells. Transfection of Dyn K44A alone did not alter the surface levels of β1 integrin or MHC1 (data not shown). However, Sullivan *et. al* reported that transfection of dominant negative dynamin reduced nearly half of the down-regulation of αV integrin and a significant portion of the down-regulation of MHC1 by GP (Sullivan et al., 2005). In contrast, we found that after co-transfection of DNA encoding Dyn K44A and GP in a ratio of 3:1, no change in the down-regulation of MHC1 or β1 integrin could be observed

(Fig 5C). It should be noted that the transfection efficiency of GP in these experiments varied by less than 2% between samples (Fig 5C, upper left-hand quadrants). We also examined the effect of Dyn K44A on the down-regulation of β1 integrin and MHC1 by Tva-muc. Transfections were performed as with GP. Our data indicate that Dyn K44A does not reduce the number of cells in Tva-muc transfected cultures that have down-regulated levels of β1 integrin and MHC1 (Fig. 5D).

We have previously reported that in cultures transfected with GP, floating cells are 90% positive for GP expression and 95% viable (Simmons et al., 2002). Here we demonstrate that floating cells also exhibited the most dramatic phenotype of surface protein down-regulation (Fig. 5E). To ensure that cells co-transfected with GP and Dyn K44A expressed Dyn K44A, floating cells were also analyzed by intracellular staining for dynamin I. Flow cytometry revealed that 95% of floating cells stained positive for dynamin I (Fig. 5F).

Discussion

The mucin domain of Ebola GP has no apparent critical function in entry or fusion mediated by the glycoprotein, but instead decreases binding to target cells and lowers the efficiency of infection (Kaletsky, Simmons, and Bates, 2007; Manicassamy et al., 2005; Medina et al., 2003). Despite this fact, there appears to be selective pressure to maintain this domain and conserve both the overall length and level of glycosylation suggesting that this portion of the viral glycoprotein plays an important role in other aspects of the viral infection cycle *in vivo*. Within the architecture of the Ebola glycoprotein trimer, the mucin domain is in a position to interact with other cellular surface proteins or protect the rest of GP from immune recognition (Lee et al., 2008).

A number of laboratories have observed that expression of Ebola GP alone can cause cytopathic effects and down modulation of surface proteins in numerous types of cultured cells and in isolated blood vessels (Chan, Ma, and Goldsmith, 2000; Simmons et al., 2002; Takada et al., 2000; Yang et al., 2000). A recent report by Alazard-Dany *et al*. demonstrated that similar effects are seen upon infection of cells with Ebola virus. Analysis of infected cells demonstrated that moderate to low levels of GP expression seen early in infection do not induce cell rounding; this is in agreement with our data, which indicates that 293T cells down-regulate surface proteins after reaching a threshold of surface GP expression (Fig. 4A, B). However, cell rounding, detachment, and the down-regulation of β1 integrin and MHC1 can be observed by 48 hours post-infection with Ebola virus, suggesting that the effects seen are not an artifact of over-expressing GP *in vitro* (Alazard-Dany et al., 2006).

The data presented here demonstrate that the mucin domain of Ebola Zaire is sufficient to cause cytopathic effects that are comparable with those caused by full-length Ebola GP. Tva-muc induces cell rounding and detachment in 293T cells and significant surface down-regulation of both β1 integrin and MHC1. Previous studies indicate that, depending upon cell type, other cell surface proteins can also be down-regulated by Ebola GP expression (Simmons et al., 2002). Although not studied here, it seems likely that the isolated mucin domain would similarly down-modulate these other cellular proteins.

The extent to which the GP-induced alteration of cellular morphology and physiology contribute to viral pathogenesis remain to be tested; however, GP-induced cytopathology may have several effects. Fatal Ebola infection is characterized by an aberrant innate immune response with little or no adaptive immune response. This ineffective immune response permits high rates of Ebola viral replication in many tissues including liver, spleen, and kidneys (reviewed in (Zampieri, Sullivan, and Nabel, 2007). Non-human primate studies demonstrated that monocytes, macropahge and dendritic cells are primary targets of Ebola infection (Geisbert

et al., 2003a) and have revealed that the innate immune response and resulting communication of antigen-presenting cells (APCs) to the adaptive arm of the immune system is disrupted during Ebola infection (reviewed in (Mahanty and Bray, 2004). Effects of GP-mediated cytopathology on APCs could contribute to immune dysregulation. We have previously demonstrated that GP expression causes rounding in macrophages (Simmons et al., 2002). Integrins are known to play a critical role in the homing of leukocytes to sites of infection (Butcher, 1991), therefore loss of adhesion may disrupt the function of macrophages or dendritic cells. Additionally, the down-regulation of MHC1 in other cell types could be a mechanism of escape from $CD8^+$ T-cell surveillance. Furthermore, loss of adhesion induced by GP expression in cultured saphenous veins is thought to be a model for hemorrhagic symptoms seen during Ebola infection (Sullivan et al., 2005; Yang et al., 2000). Finally, loss of adhesion by Ebola GP has been shown to cause anoikis in primary endothelial cells (Ray et al., 2004). GP-induced loss of adhesion and resulting anoikis could provide one mechanism for necrosis seen during infection, specifically in organs such as the liver where viral replication is high and immune infiltration is limited, though other cellular factors such as tumor necrosis factor-related apoptosis-inducing ligand have also been implicated in necrotic cell death (Geisbert et al., 2003a; Geisbert et al., 2003b).

If the effects of the mucin domain contribute to the pathogenesis of the Zaire subtype of Ebola virus, one might expect cytopathology caused by the less-pathogenic Reston subtype to be measurably less. Indeed, our previous report comparing Ebola GP Zaire and Reston found that GP Reston expression caused not as much cell detachment and less loss of surface staining of integrins and MHC1 by flow cytometry (Simmons et al., 2002). In contrast, comparison of chimeric proteins carrying the isolated mucin domain from either Reston or Zaire GP indicates that both are equal in their ability to cause cytopathology. This observation might indicate that the mucin domain does not determine or significantly influence the pathogenic potential of Ebola. Alternatively, these findings may suggest that the presentation of the mucin domain in the context of the full glycoprotein regulates the ability of the domain to cause cytopathology.

It is also interesting that, while the mucin domain normally induces the rounding phenotype from within the GP trimer, we have demonstrated that it is able to exert these effects from within the monomeric protein, Tva. When the mucin domain of GP is expressed in the context of the GPI-anchored isoform of Tva, the rounding phenotype is abolished and protein down-regulation of MHC1 and β1 integrin is not observed. It is possible that the mucin domain in GPI Tva-muc is physically positioned or becomes differentially glycosylated in such a way that prevents rounding. A more appealing alternative is that GPI Tva traffics or is localized at the plasma membrane differently than Tva. Immunofluorescence of these constructs in HeLa cells shows possible differences in internal staining, but does not reveal any discernable difference in plasma membrane staining (Fig. 1C). However, it has been reported that GPI Tva localizes to detergent-resistant membranes, while Tva does not, and that GPI Tva traffics to an acidic compartment through a different endocytic pathway than Tva upon binding of ASLV (Narayan, Barnard, and Young, 2003). These characteristics could explain the differences between Tva-muc and GPI Tva-muc.

The mechanism by which Ebola GP causes cellular cytopathology is also unknown. A recent report suggests that GP utilizes a dynamin-dependent pathway to cause surface protein down-regulation (Sullivan et al., 2005). Dynamin has been implicated in vesicle fission for several pathways, including clathrin- dependent and independent endocytosis, as well as *trans*-Golgi budding (Jones et al., 1998; Oh, McIntosh, and Schnitzer, 1998; van der Bliek et al., 1993). Therefore, it is possible that GP alters surface protein levels by affecting endocytosis. We addressed the function of dynamin in the process of GP- and Tva-muc- mediated surface protein down-regulation. As demonstrated in Figure 5, a dominant negative version of dynamin I effectively blocked endocytosis of the transferrin receptor, but could not block the down-

regulation of β1 integrin or MHC1 by Ebola GP or the chimeric Tva-muc protein. Thus, we propose a model of down-regulation that is independent of dynamin-regulated pathways.

The two surface proteins studied here, β1 integrin and MHC1, both undergo constant endocytosis and recycling back to the plasma membrane (Bretscher, 1989; Bretscher, 1992; Mahmutefendic et al., 2006; Reid and Watts, 1990). Many viruses encode proteins that modulate MHC1 levels at the cell surface. For example, the K3 and K5 proteins from Kaposi's sarcoma-associated herpesvirus increase the rate of MHC1 endocytosis (Coscoy and Ganem, 2000). Other viruses block MHC1 expression by interfering in the ER. The US11 gene encoded by the human cytomegalovirus retro-translocates newly synthesized MHC1 molecules out of the ER where they are degraded by the proteosome (Wiertz et al., 1996). Furthermore, some viral proteins are able to modulate MHC1 levels by influencing multiple pathways. The Nef protein from HIV has been reported to increase endocytosis of MHC1 and also to redirect newly-sythesized MHC1 from the *trans*-Golgi network (TGN) to the lysosome (Kasper and Collins, 2003; Roeth et al., 2004; Schwartz et al., 1996). Therefore, it seemed prudent to ask whether Ebola GP could cause rounding and protein down-regulation when restricted to the ER. As shown in Figures 3 and 4, our findings reject a model of down-regulation of β1 integrin and MHC1 by interference in the ER. These data suggest a mechanism of regulation at the plasma membrane or TGN.

GP directs the down-regulation of surface proteins, but also appears to down-regulate its own surface expression in a manner that seems concurrent with that of β1 integrin and MHC1 (Fig. 4A, B). Because the mechanism of action is unknown, it is not clear if GP plays a direct role in guiding the down-regulation of other surface molecules. It has, however, been reported that GP and αV integrin, which is also down-regulated in 293T cells, can be co-immunoprecipitated (Sullivan et al., 2005). If GP directly binds to proteins to facilitate down-regulation, this could explain the observation that cells showing down-modulation of β1 integrin or MHC1 have reduced surface levels of GP (Fig. 4). Interestingly, Tva-muc is able to down-regulate β1 integrin and MHC1 without a reduction in surface expression of Tva-muc (Fig. 2A, B). This could indicate that the mechanism of down-regulation is indirect, such as through a signaling cascade which affects endocytosis and/or recycling. Alternatively, it is possible that Tva-muc interacts directly with β1 integrin and MHC1, but simply recycles back to the plasma membrane more efficiently than GP. Additional experiments analyzing the mechanism of downmodulation are required to distinguish these possibilities.

Overall, the data presented here suggests that the mucin domain within Ebola GP acts at the cell surface to affect cellular adhesion and down modulate surface protein expression by a mechanism that does not require dynamin dependent endocytosis. The role of these GP-mediated effects in the pathogenesis of Ebola virus in primates is uncertain, however cellular loss of adhesion may play a role cell death by anoikis, hemorrhagic symptoms, and in combination with reduction in levels of immune regulatory proteins such as MHC1, likely contributes to immune evasion by Ebola virus.

Materials and Methods

Plasmids, cell culture, and transfections

Tva constructs were created by using two isoforms of the quail Tva ORF, Tva950 and Tva800 (Bates, Young, and Varmus, 1993). The transmembrane (Tva950) and GPI-anchored (Tva800) isoforms of Tva used here have the accession numbers L22753 and L22752, respectively. For each isoform, the mucin domain from the Zaire subtype (Mayinga strain) of the Ebola virus glycoprotein (amino acids 312–462) or Reston subtype (amino acids 317–478) was cloned between residues 77 and 78 of Tva. At the C-terminal end of the mucin domain, a flexible three amino acid linker, AAV, or PAV was added just before Tva amino acid 78 for the Zaire and

Reston subtypes, respectively. To create an ER-retained version of Ebola GP, cDNA encoding the membrane-anchored form of Ebola GP (Mayinga strain, accession number U23187) was used. The four amino acid tag, KKMP, was appended to the C-terminus of the GP ORF. Constructs were cloned into the pCAGGS expression vector, except where indicated. Amino acid positions stated here are counted from the initial methionine. The dominant negative version of dynamin I (Dyn K44A) was a gift from Sandra Schmid (Damke et al., 1994). The coding region for Dyn K44A was removed from its original vector by EcoRI and XbaI digest and cloned into a pcDNA3.1+ backbone to create a mammalian expression vector.

All cells were cultured in DMEM (Gibco) with 10% bovine cosmic-calf serum (HyClone) and penicillin/streptomycin (Gibco) at 37 °C with 5% CO_2. For flow cytometry, fluorescence microscopy, and western blotting, 293T cells were plated at ~8×10^5 cells per well in 6-well plates one day prior to transfection. Cells were transiently transfected by calcium-phosphate precipitation with 6 μg DNA per well unless otherwise stated. Cells to be visualized with GFP were co-transfected with an additional 2 μg cDNA encoding eGFP. For enumeration of floating cells, 10 cm plates were plated with 4.5×10^6 293T cells one day prior to transfection; cells were transiently transfected with 30 μg DNA encoding GP or Tva constructs and 10 μg DNA encoding eCFP. Immunofluorescence was performed using HeLa cells that were plated on glass coverslips at 6×10^4 cells per coverslip in 24-well plates one day prior to transfection. HeLa cells were transiently transfected by calcium-phosphate precipitation with 1.5 μg DNA per coverslip. For all transfections, media was replaced 5 hours post-transfection.

Floating cell assay

24 hours after transfection, supernatants were removed and combined with 2 ml PBS that had been used to gently wash the monolayer. An aliquot of the sample was employed to determine cell concentration and total sample volume was measured. Only CFP positive cells were counted using an improved Neubauer hemocytometer (Reichert) on an Nikon TE300 inverted fluorescent microscope. FACS analysis demonstrated that >95% of the CFP positive cells also express the co-transfected GP-encoding plasmid. Percent non-adherent cells were calculated as: non-adherent cells/(adherent + non-adherent cells) × 100%. All experiments were performed in triplicate.

Cell lysates and western blotting

Transfected cells were removed by resuspension in the culturing media. Cells were pelleted at 4 °C for 5 min at 1300 × g. Pellets were resuspended in RIPA buffer with complete protease inhibitor cocktail (Roche) for 5 minutes on ice or at room temperature. Lysates were cleared by centrifugation at 4 °C for 5 minutes at 20,800 × g. 30 μl samples were mixed with reducing SDS buffer, boiled for 5 minutes, and separated on a 4–15% Criterion PAGE gel (Bio-Rad). Proteins were transferred to PVDF (Millipore) at a 400 mA constant current. Membranes were blocked in 5% milk in TBS or 3% BSA in TBST for 45 minutes or overnight. Membranes were probed with rabbit polyclonal anti-GP sera (Lin et al., 2003), rabbit polyclonal anti-Tva sera (Bates, Young, and Varmus, 1993), or mouse anti-dynamin I MAb (clone 41, BD Transduction Labs) in blocking buffer. Protein was detected with stabilized goat anti-rabbit or anti-mouse HRP conjugated antibodies (Pierce) in blocking buffer for 45 minutes. Membranes were visualized with SuperSignal Femto substrate (Pierce).

Endoglycosidase assay

30 μl of each 293T cell lysate was incubated with denaturing buffer (NEB) for 10 minutes at 60 °C. Samples were then incubated with buffer alone (G7 and NP40, NEB), PNGase F, or Endo H_f plus appropriate buffers (NEB) for 4 to 6 hours at 37 °C. Samples were then separated by SDS-PAGE and blotted as described above.

Transferrin uptake assay

HeLa cells were plated at 1×10^5 cells per coverslip in a 24-well plate format. Cells were transfected with Lipofectamine 2000 (Invitrogen) according to manufacturer's instructions with 1.5 μg per well of Dyn K44A or empty pcDNA3.1 vector. At 22 hrs post transfection, media was removed and replaced with DMEM lacking serum. At 24 hrs post transfection, cells were placed on ice for 10 min. Human transferrin conjugated to Alexa Fluor 594 (Invitrogen) was added to a final concentration of 100 μg/ml and incubated on ice for 30 min. Cells were then washed 3 times with ice-cold PBS and either immediately fixed (T=0) or incubated with DMEM + 10% serum at 37 °C for 15, 30, or 60 min, then fixed. Cells were then stained for dynamin I as described later.

Flow cytometry

293T cells were detached from the TC plate 24 hours post transfection with PBS −/−, 0.5 mM EDTA and combined with well media. Cells were pelleted at 4 °C for 5 min at 250 × g, then resuspended in wash buffer (PBS with 1% bovine calf serum and 0.05% NaAzide) and aliquoted for staining. For detection of Ebola GP, cells were stained with the human MAb, KZ52 (Maruyama et al., 1999) and detected with FITC anti-human IgG (PharMingen). For detection of Tva proteins, cells were stained with rabbit polyclonal anti-Tva sera (Bates, Young, and Varmus, 1993) and detected with FITC goat anti-rabbit IgG (Rockland). For detection of β1-integrin, cells were co-stained with anti-human CD29 PE-Cy5 conjugate (eBioscience); for detection of MHC-1, cells were co-stained with anti- HLA-ABC PE-Cy5 conjugate (eBioscience). For intracellular dynamin I staining, cells were permeabilized using Cytofix/Cytoperm (BD Biosciences) for 20 min, followed by washing with Permwash (BD Biosciences). For detection of dynamin I, cells were stained with mouse anti-dynamin Mab (clone 41, BD Transduction Labs) and detected with anti-mouse Alexa Fluor 488 antibodies (Invitrogen) in Permwash buffer. All staining was performed on ice for 1 hour, followed by washing. Live cell gates were drawn based on forward and side scatter. For each sample, 10,000 events in the live cell gate were analyzed. Data were collected on a Becton Dickinson FACSCalibur and analyzed using FlowJo software (Tree Star, Inc.).

Immunofluorescence

At 48 hours post-transfection, media was removed, cells were washed with PBS, and fixed with 3% PFA in PBS for 20 minutes. Cells were then washed with PBS, then permeabilized with 0.2% saponin, 1% goat serum in PBS for 5 minutes, then washed with PBS. Cells were blocked with 10% goat serum, 0.1% Tween-20 in PBS for 2 hours. For GP and ER staining, coverslips were incubated with mouse anti-Ebola GP MAb (gift from Yoshihiro Kawaoka) and rabbit anti-calnexin (StressGen) and detected with goat anti- mouse or rabbit Alexa Fluor 594 or 488 antibodies, respectively (Invitrogen). For Golgi staining, cells were re-blocked with 10% mouse sera, then probed with mouse MAb FITC anti-GM 130 (BD Transduction Labs). For Tva staining, coverslips were incubated with rabbit polyclonal anti-Tva sera and detected with anti-rabbit Alexa Fluor 594 antibodies (Invitrogen). For dynamin I staining, coverslips were incubated with mouse anti-dynamin I MAb (clone 41, BD Transduction Labs) and detected with anti-mouse Alexa Fluor 488 antibodies (Invitrogen). Cells were washed with PBS after each staining step. For non-permeabilizing conditions, cells were fixed with 1% PFA in PBS for 20 minutes, washed, then blocked with 10% goat serum in PBS and stained as described above. All coverslips were mounted on glass slides with mounting medium containing DAPI (Vectasheild). Z-section images were collected on a Leica DMRE fluorescence microscope using Open Lab software (Improvision). Thirty z-sections per image were collected at 0.2 μm intervals. Z-section data were deconvoluted using Velocity software (Improvision) to a 98% confidence level or 15 iterations. Images shown are single, deconvoluted, z-sections except where indicated.

Acknowledgements

The authors would like to thank Andrew Piefer for assistance with fluorescence microscopy and manuscript comments, Rachel Kaletsky for manuscript comments, Dennis Burton for providing the KZ52 antibody, Sandra Schmid for the dynamin I K44A construct, and Yoshihiro Kawaoka for providing anti-GP monoclonal antibodies for IF. This work was funded by Public Health Service grants T32-GM07229 and T32-AI55400 (JF), T32-AI07324 (MM), and R01-AI43455 (PB).

References

Alazard-Dany N, Volchkova V, Reynard O, Carbonnelle C, Dolnik O, Ottmann M, Khromykh A, Volchkov VE. Ebola virus glycoprotein GP is not cytotoxic when expressed constitutively at a moderate level. J Gen Virol 2006;87(Pt 5):1247–57. [PubMed: 16603527]

Barrientos LG, Rollin PE. Release of cellular proteases into the acidic extracellular milieu exacerbates Ebola virus-induced cell damage. Virology. 2006

Bates P, Young JA, Varmus HE. A receptor for subgroup A Rous sarcoma virus is related to the low density lipoprotein receptor. Cell 1993;74(6):1043–51. [PubMed: 8402880]

Beck M, Strand MR. Glc1.8 from Microplitis demolitor bracovirus induces a loss of adhesion and phagocytosis in insect high five and S2 cells. J Virol 2005;79(3):1861–70. [PubMed: 15650210]

Bretscher MS. Endocytosis and recycling of the fibronectin receptor in CHO cells. Embo J 1989;8(5): 1341–8. [PubMed: 2527741]

Bretscher MS. Circulating integrins: alpha 5 beta 1, alpha 6 beta 4 and Mac-1, but not alpha 3 beta 1, alpha 4 beta 1 or LFA-1. Embo J 1992;11(2):405–10. [PubMed: 1531629]

Butcher EC. Leukocyte-endothelial cell recognition: three (or more) steps to specificity and diversity. Cell 1991;67(6):1033–6. [PubMed: 1760836]

Chan SY, Ma MC, Goldsmith MA. Differential induction of cellular detachment by envelope glycoproteins of Marburg and Ebola (Zaire) viruses. J Gen Virol 2000;81(Pt 9):2155–9. [PubMed: 10950971]

Coscoy L, Ganem D. Kaposi's sarcoma-associated herpesvirus encodes two proteins that block cell surface display of MHC class I chains by enhancing their endocytosis. Proc Natl Acad Sci U S A 2000;97(14):8051–6. [PubMed: 10859362]

Damke H, Baba T, Warnock DE, Schmid SL. Induction of mutant dynamin specifically blocks endocytic coated vesicle formation. J Cell Biol 1994;127(4):915–34. [PubMed: 7962076]

Fisher-Hoch SP, Brammer TL, Trappier SG, Hutwagner LC, Farrar BB, Ruo SL, Brown BG, Hermann LM, Perez-Oronoz GI, Goldsmith CS, et al. Pathogenic potential of filoviruses: role of geographic origin of primate host and virus strain. Journal of Infectious Diseases 1992;166(4):753–63. [PubMed: 1527410]

Geisbert TW, Hensley LE, Larsen T, Young HA, Reed DS, Geisbert JB, Scott DP, Kagan E, Jahrling PB, Davis KJ. Pathogenesis of Ebola Hemorrhagic Fever in Cynomolgus Macaques: Evidence that Dendritic Cells Are Early and Sustained Targets of Infection. Am J Pathol 2003a;163(6):2347–2370. [PubMed: 14633608]

Geisbert TW, Young HA, Jahrling PB, Davis KJ, Larsen T, Kagan E, Hensley LE. Pathogenesis of Ebola Hemorrhagic Fever in Primate Models: Evidence that Hemorrhage Is Not a Direct Effect of Virus-Induced Cytolysis of Endothelial Cells. Am J Pathol 2003b;163(6):2371–2382. [PubMed: 14633609]

Jones SM, Howell KE, Henley JR, Cao H, McNiven MA. Role of dynamin in the formation of transport vesicles from the trans-Golgi network. Science 1998;279(5350):573–7. [PubMed: 9438853]

Kaletsky RL, Simmons G, Bates P. Proteolysis of the Ebola virus glycoproteins enhances virus binding and infectivity. J Virol 2007;81(24):13378–84. [PubMed: 17928356]

Kasper MR, Collins KL. Nef-mediated disruption of HLA-A2 transport to the cell surface in T cells. J Virol 2003;77(5):3041–9. [PubMed: 12584329]

Lee JE, Fusco ML, Hessell AJ, Oswald WB, Burton DR, Saphire EO. Structure of the Ebola virus glycoprotein bound to an antibody from a human survivor. Nature 2008;454(7201):177–82. [PubMed: 18615077]

Lin G, Simmons G, Pohlmann S, Baribaud F, Ni H, Leslie GJ, Haggarty BS, Bates P, Weissman D, Hoxie JA, Doms RW. Differential N-linked glycosylation of human immunodeficiency virus and Ebola

virus envelope glycoproteins modulates interactions with DC-SIGN and DC-SIGNR. J Virol 2003;77 (2):1337–46. [PubMed: 12502850]

Mahanty S, Bray M. Pathogenesis of filoviral haemorrhagic fevers. The Lancet Infectious Diseases 2004;4(8):487–498. [PubMed: 15288821]

Mahmutefendic H, Blagojevic G, Kucic N, Lucin P. Constitutive internalization of murine MHC class I molecules. J Cell Physiol. 2006

Manicassamy B, Wang J, Jiang H, Rong L. Comprehensive analysis of ebola virus GP1 in viral entry. J Virol 2005;79(8):4793–805. [PubMed: 15795265]

Maruyama T, Rodriguez LL, Jahrling PB, Sanchez A, Khan AS, Nichol ST, Peters CJ, Parren PW, Burton DR. Ebola virus can be effectively neutralized by antibody produced in natural human infection. J Virol 1999;73(7):6024–30. [PubMed: 10364354]

McGuckin MA, Walsh MD, Hohn BG, Ward BG, Wright RG. Prognostic significance of MUC1 epithelial mucin expression in breast cancer. Hum Pathol 1995;26(4):432–9. [PubMed: 7705823]

Medina MF, Kobinger GP, Rux J, Gasmi M, Looney DJ, Bates P, Wilson JM. Lentiviral vectors pseudotyped with minimal filovirus envelopes increased gene transfer in murine lung. Mol Ther 2003;8(5):777–89. [PubMed: 14599811]

Narayan S, Barnard RJ, Young JA. Two retroviral entry pathways distinguished by lipid raft association of the viral receptor and differences in viral infectivity. J Virol 2003;77(3):1977–83. [PubMed: 12525631]

Oh P, McIntosh DP, Schnitzer JE. Dynamin at the neck of caveolae mediates their budding to form transport vesicles by GTP-driven fission from the plasma membrane of endothelium. J Cell Biol 1998;141(1):101–14. [PubMed: 9531551]

Osako M, Yonezawa S, Siddiki B, Huang J, Ho JJ, Kim YS, Sato E. Immunohistochemical study of mucin carbohydrates and core proteins in human pancreatic tumors. Cancer 1993;71(7):2191–9. [PubMed: 8384065]

Ray RB, Basu A, Steele R, Beyene A, McHowat J, Meyer K, Ghosh AK, Ray R. Ebola virus glycoprotein-mediated anoikis of primary human cardiac microvascular endothelial cells. Virology 2004;321(2): 181–188. [PubMed: 15051379]

Reid PA, Watts C. Cycling of cell-surface MHC glycoproteins through primaquine-sensitive intracellular compartments. Nature 1990;346(6285):655–7. [PubMed: 2166918]

Roeth JF, Williams M, Kasper MR, Filzen TM, Collins KL. HIV-1 Nef disrupts MHC-I trafficking by recruiting AP-1 to the MHC-I cytoplasmic tail. J Cell Biol 2004;167(5):903–13. [PubMed: 15569716]

Sanchez, A.; Khan, AS.; Zaki, SR.; Nabel, GJ.; Ksiazek, TG.; Peters, CJ. Filoviridae: Marburg and Eboila Viruses. In: Knipe, DM.; Howley, PM.; Griggen, DE.; Lamb, RA.; Martin, MA.; Roizman, B.; Straus, SE., editors. Fields Virology. Vol. 1. Lippincott, Williams & Wilkins; 2001. p. 1279-1304.2 vols

Sanchez A, Trappier SG, Mahy BW, Peters CJ, Nichol ST. The virion glycoproteins of Ebola viruses are encoded in two reading frames and are expressed through transcriptional editing. Proceedings of the National Academy of Sciences of the United States of America 1996;93(8):3602–7. [PubMed: 8622982]

Sanchez A, Yang ZY, Xu L, Nabel GJ, Crews T, Peters CJ. Biochemical analysis of the secreted and virion glycoproteins of Ebola virus. J Virol 1998;72(8):6442–7. [PubMed: 9658086]

Schwartz O, Marechal V, Le Gall S, Lemonnier F, Heard JM. Endocytosis of major histocompatibility complex class I molecules is induced by the HIV-1 Nef protein. Nat Med 1996;2(3):338–42. [PubMed: 8612235]

Simmons G, Wool-Lewis RJ, Baribaud F, Netter RC, Bates P. Ebola virus glycoproteins induce global surface protein down-modulation and loss of cell adherence. J Virol 2002;76(5):2518–28. [PubMed: 11836430]

Sullivan NJ, Peterson M, Yang ZY, Kong WP, Duckers H, Nabel E, Nabel GJ. Ebola virus glycoprotein toxicity is mediated by a dynamin-dependent protein-trafficking pathway. J Virol 2005;79(1):547–53. [PubMed: 15596847]

Takada A, Watanabe S, Ito H, Okazaki K, Kida H, Kawaoka Y. Downregulation of beta1 integrins by Ebola virus glycoprotein: implication for virus entry. Virology 2000;278(1):20–6. [PubMed: 11112476]

van der Bliek AM, Redelmeier TE, Damke H, Tisdale EJ, Meyerowitz EM, Schmid SL. Mutations in human dynamin block an intermediate stage in coated vesicle formation. J Cell Biol 1993;122(3): 553–63. [PubMed: 8101525]

Volchkov VE, Feldmann H, Volchkova VA, Klenk HD. Processing of the Ebola virus glycoprotein by the proprotein convertase furin. Proc Natl Acad Sci U S A 1998;95(10):5762–7. [PubMed: 9576958]

Volchkov VE, Volchkova VA, Muhlberger E, Kolesnikova LV, Weik M, Dolnik O, Klenk HD. Recovery of infectious Ebola virus from complementary DNA: RNA editing of the GP gene and viral cytotoxicity. Science 2001;291(5510):1965–9. [PubMed: 11239157]

Volchkova VA, Feldmann H, Klenk HD, Volchkov VE. The nonstructural small glycoprotein sGP of Ebola virus is secreted as an antiparallel-orientated homodimer. Virology 1998;250(2):408–14. [PubMed: 9792851]

Wesseling J, van der Valk SW, Hilkens J. A mechanism for inhibition of E-cadherin-mediated cell-cell adhesion by the membrane-associated mucin episialin/MUC1. Mol Biol Cell 1996;7(4):565–77. [PubMed: 8730100]

Wesseling J, van der Valk SW, Vos HL, Sonnenberg A, Hilkens J. Episialin (MUC1) overexpression inhibits integrin-mediated cell adhesion to extracellular matrix components. J Cell Biol 1995;129(1): 255–65. [PubMed: 7698991]

Wiertz EJ, Jones TR, Sun L, Bogyo M, Geuze HJ, Ploegh HL. The human cytomegalovirus US11 gene product dislocates MHC class I heavy chains from the endoplasmic reticulum to the cytosol. Cell 1996;84(5):769–79. [PubMed: 8625414]

Yamashita K, Yonezawa S, Tanaka S, Shirahama H, Sakoda K, Imai K, Xing PX, McKenzie IF, Hilkens J, Kim YS, et al. Immunohistochemical study of mucin carbohydrates and core proteins in hepatolithiasis and cholangiocarcinoma. Int J Cancer 1993;55(1):82–91. [PubMed: 8393843]

Yang ZY, Duckers HJ, Sullivan NJ, Sanchez A, Nabel EG, Nabel GJ. Identification of the Ebola virus glycoprotein as the main viral determinant of vascular cell cytotoxicity and injury. Nat Med 2000;6 (8):886–9. [PubMed: 10932225]

Zampieri CA, Sullivan NJ, Nabel GJ. Immunopathology of highly virulent pathogens: insights from Ebola virus. Nat Immunol 2007;8(11):1159–64. [PubMed: 17952040]

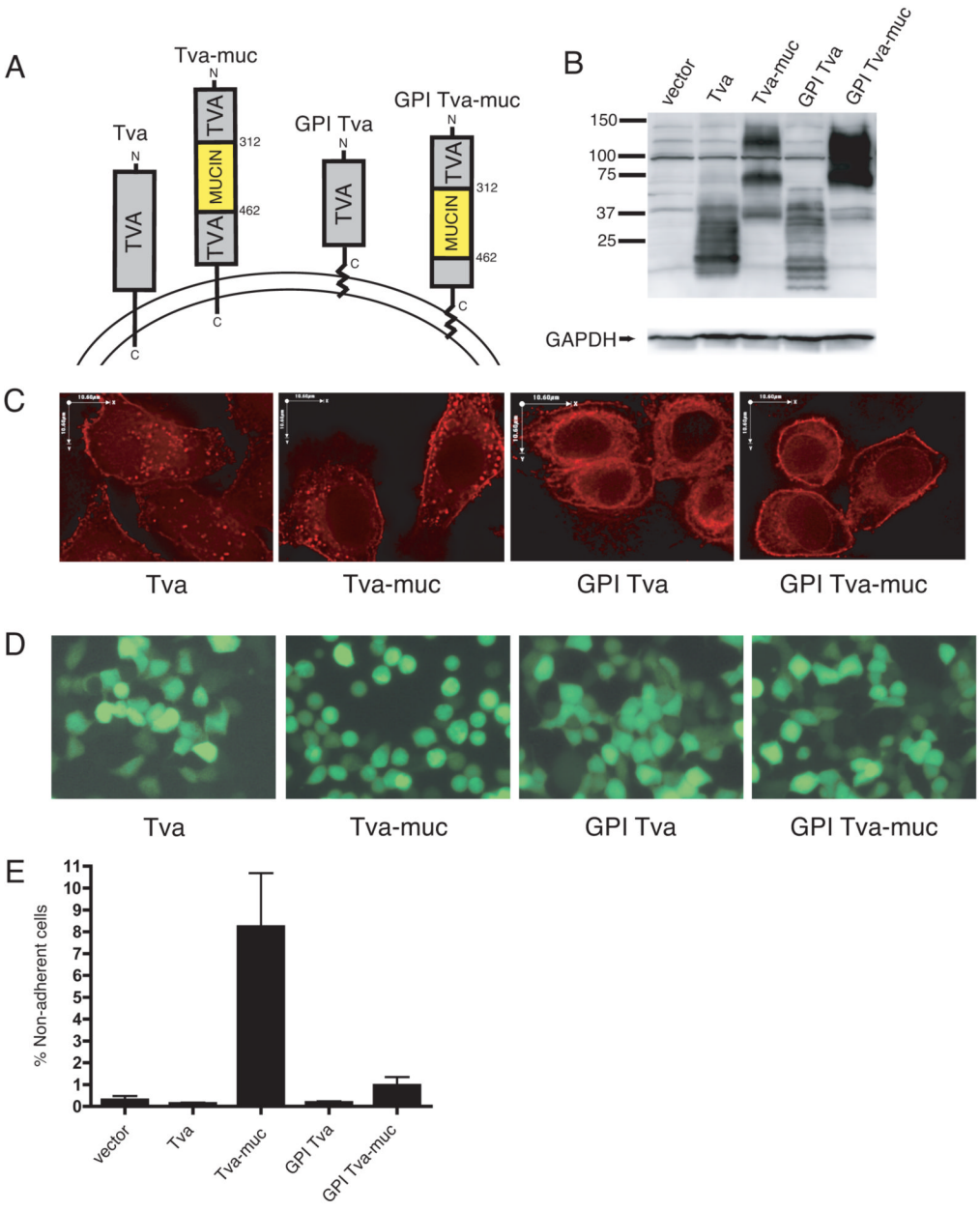

FIG. 1.

Ebola virus GP-mucin domain is sufficient to induce cell rounding and detachment. (A) Diagram of Tva constructs used to express Ebola Zaire GP-mucin domain. Numbers indicate amino acid position starting from the initial methionine. (B) 239T cells were transfected with pCAGGS alone (vector) or pCAGGS encoding the Tva constructs described in (A). Lysates were harvested in RIPA buffer after 24 h and subjected to SDS-4 to 15% PAGE, transferred to PVDF, and immunoblotted with polyclonal rabbit anti-Tva sera or GAPDH-specific monoclonal antibodies on blots run in parallel. (C) HeLa cells were transfected with Tva constructs. 48 h posttransfection, cells were fixed, permeabilized, and stained for Tva with polyclonal rabbit anti-Tva sera followed by Alexa 594 conjugated antibodies. Z-sections were captured on a fluorescence microscope and deconvoluted with software. Images shown are single, deconvoluted Z-sections. Scale bars are 10.6 μm. (D) 293T cells were co-transfected

with Tva constructs and a vector encoding eGFP in a 3:1 ratio. After 24 h fluorescent images were captured on an inverted microscope using a GFP filter. Fields represent findings from multiple experiments. (E) 239T cells were transfected with pCB6 vector alone or pCB6 encoding the Tva constructs described in (A) and co-transfected with a vector encoding eGFP in a 3:1 ratio. 24 h post-transfection, adherent and non-adherent cells were removed. CFP positive cells were counted; data is shown as % non-adherent cells. Graph shows mean of 3 replicates; error bars indicate SD. Results are representative of 2 independent experiments.

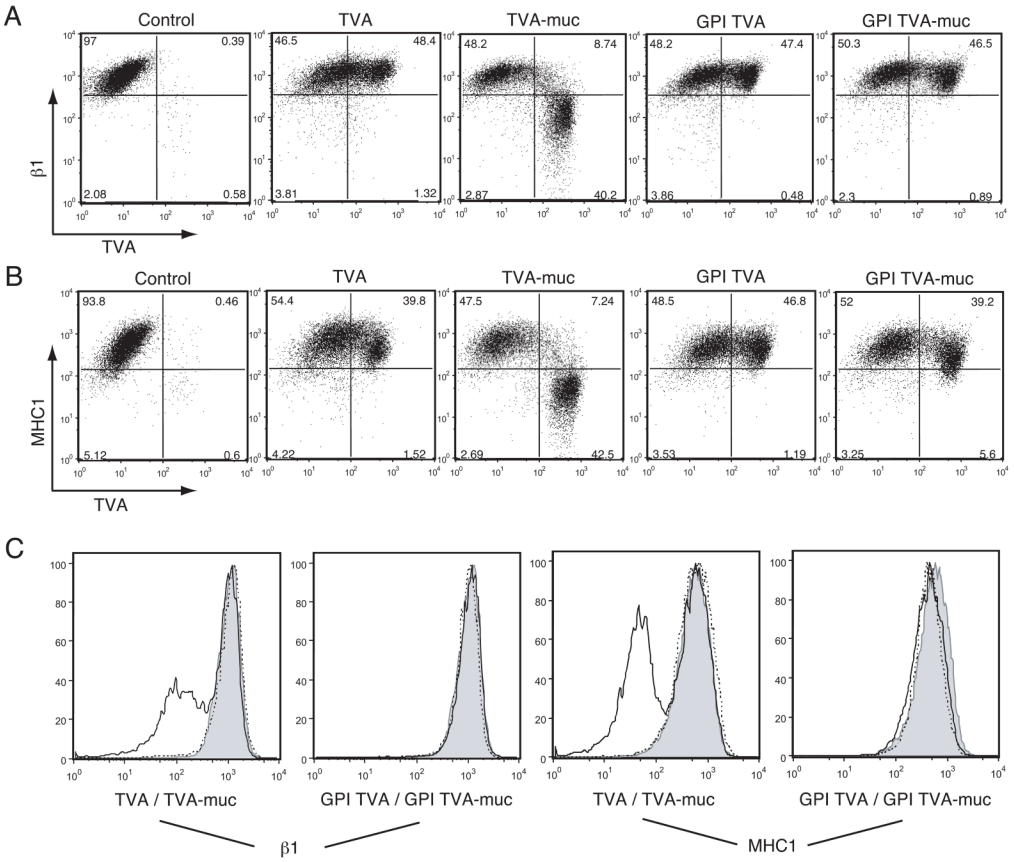

FIG. 2.

Surface protein down-regulation by Ebola GP-mucin domain. 239T cells were transfected with vector alone or vector encoding the Tva constructs described in Fig. 1A. Floating and adherent cells were harvested 24 h after transfection, pooled, and stained with polyclonal rabbit anti-Tva sera and FITC-labeled secondary antibodies, co-stained for β1 integrin or MHC1 with PE-Cy5 conjugated monoclonal antibodies and assayed by flow cytometry. Analysis is shown for events in the live cell gate. (A) β1 integrin vs. Tva surface expression. (B) MHC1 vs. Tva surface expression. (C) Histogram representation of β1 integrin surface expression (left panels) and MHC1 surface expression (right panels). Control samples are shown shaded; Tva or GPI Tva is shown as a dashed line; Tva-muc or GPI Tva-muc is shown as a solid line. Data is representative of multiple independent experiments.

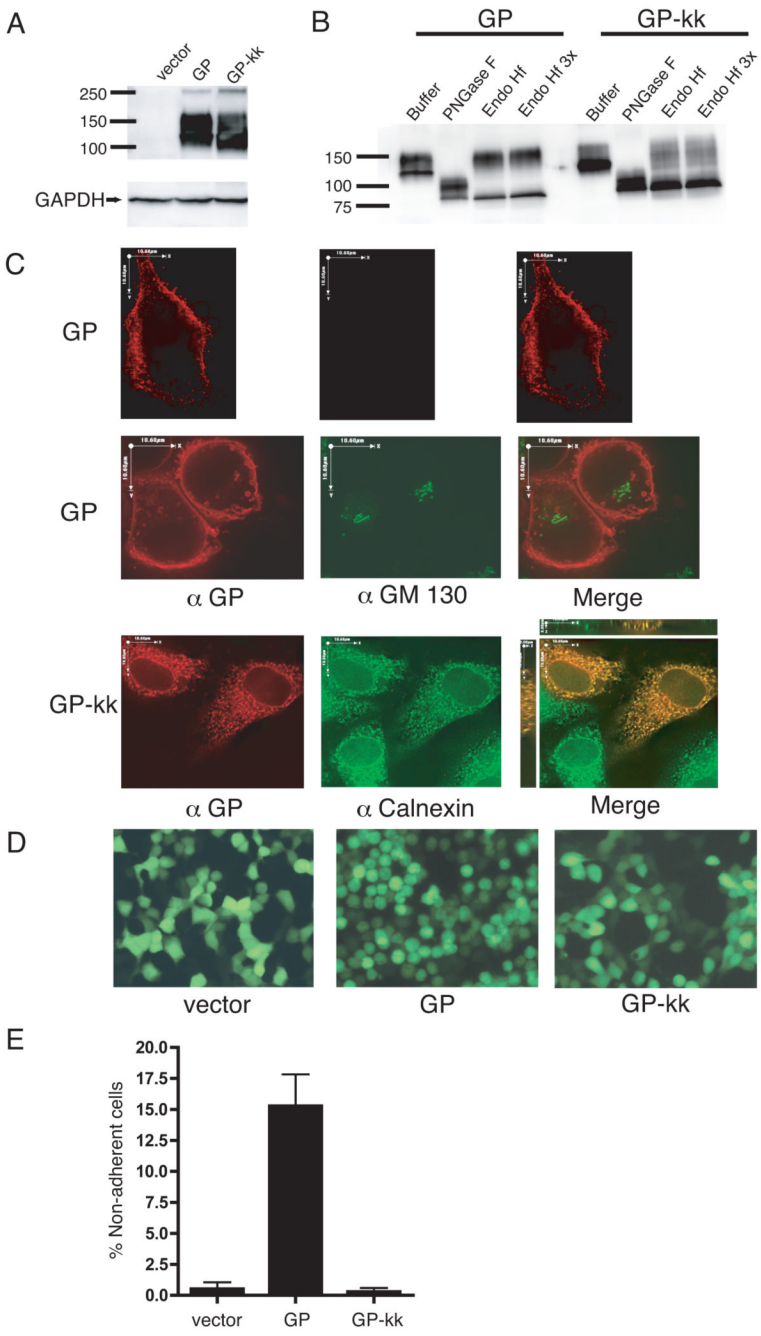

FIG. 3.

Ebola virus GP does not round cells when restricted to the ER. (A) 293T cells were transfected with vector alone, vector encoding for GP, or GP-kk (ER-restricted). Lysates were harvested in RIPA buffer after 24 h and subjected to SDS-4 to 15% PAGE, transferred to PVDF, and immunoblotted with polyclonal rabbit anti-GP sera and GAPDH-specific monoclonal antibodies. (B) GP and GP-kk lysates were denatured and incubated with enzyme buffer alone or buffer with PNGase F or Endoglycosidase H_f (at normal or 3x concentration), then subjected to SDS-PAGE and immunoblotting as described in (A). (C) HeLa cells were transfected with GP or GP-kk. 48 h posttransfection, cells were fixed, either not permeabilized (top row) or permeabilized (middle and bottom rows) and stained for GP with mouse monoclonal

antibodies, followed by Alexa 594 conjugated antibodies (red). Cells were also co-stained with FITC-conjugated monoclonal antibodies to GM 130 (green) or with rabbit polyclonal antibodies to calnexin, followed by Alexa 488 antibodies (green). Z-sections were captured on a fluorescence microscope and deconvoluted. Images shown in top and middle rows are composite, deconvoluted Z-sections. Images in the bottom row are single, deconvoluted Z-sections; the merge panel also shows views in the XZ and YZ planes. Scale bars are 10.6 μm. (D) 293T cells were transfected with vector alone, or vector encoding GP, or GP-kk and co-transfected with eGFP in a 3:1 ratio. After 24 h fluorescent images were captured on an inverted microscope using a GFP filter. Fields represent findings from multiple experiments. (E) 293T cells were transfected with vector alone or vector encoding for GP or GP-kk and co-transfected with a vector encoding eGFP in a 3:1 ratio. 24 h post-transfection, adherent and non-adherent cells were removed. CFP positive cells were counted; data is shown as % non-adherent cells. Graph shows mean of 3 replicates; error bars indicate SD. Results are representative of 2 independent experiments.

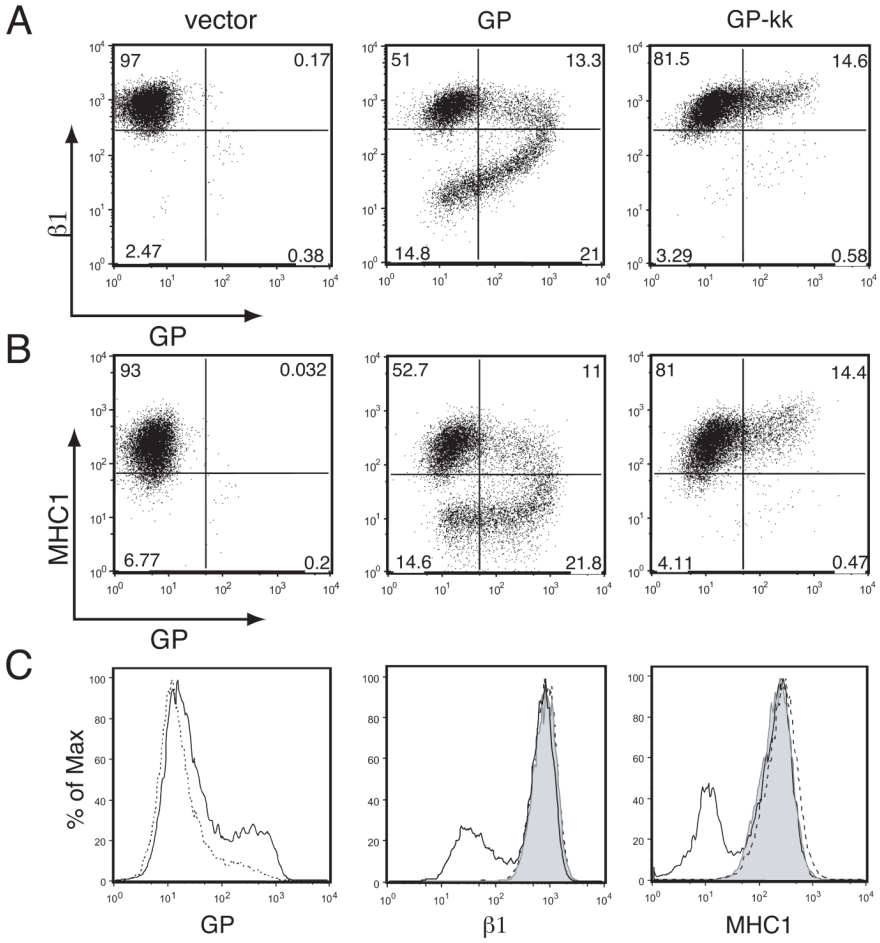

FIG. 4.

Ebola virus GP does not induce surface protein down-regulation when restricted to ER. 293T cells were transfected with vector alone or vector encoding for GP or GP-kk. Floating and adherent cells were harvested 24 h after transfection, pooled, and stained with antibodies to GP using human monoclonal antibodies and FITC-labeled secondary antibodies, co-stained for β1 integrin or MHC1 with PE-Cy5 conjugated monoclonal antibodies and assayed by flow cytometry. Analysis is shown for events in the live cell gate. (A) β1 integrin vs. GP surface expression. (B) MHC1 vs. GP surface expression. (C) Histogram representation of GP surface expression (left panel), β1 surface expression (middle panel), and MHC1 surface expression (right panel). Control samples are shown shaded; GP is shown as a solid line, and GP-kk is shown as a dashed line. Data is representative of multiple independent experiments.

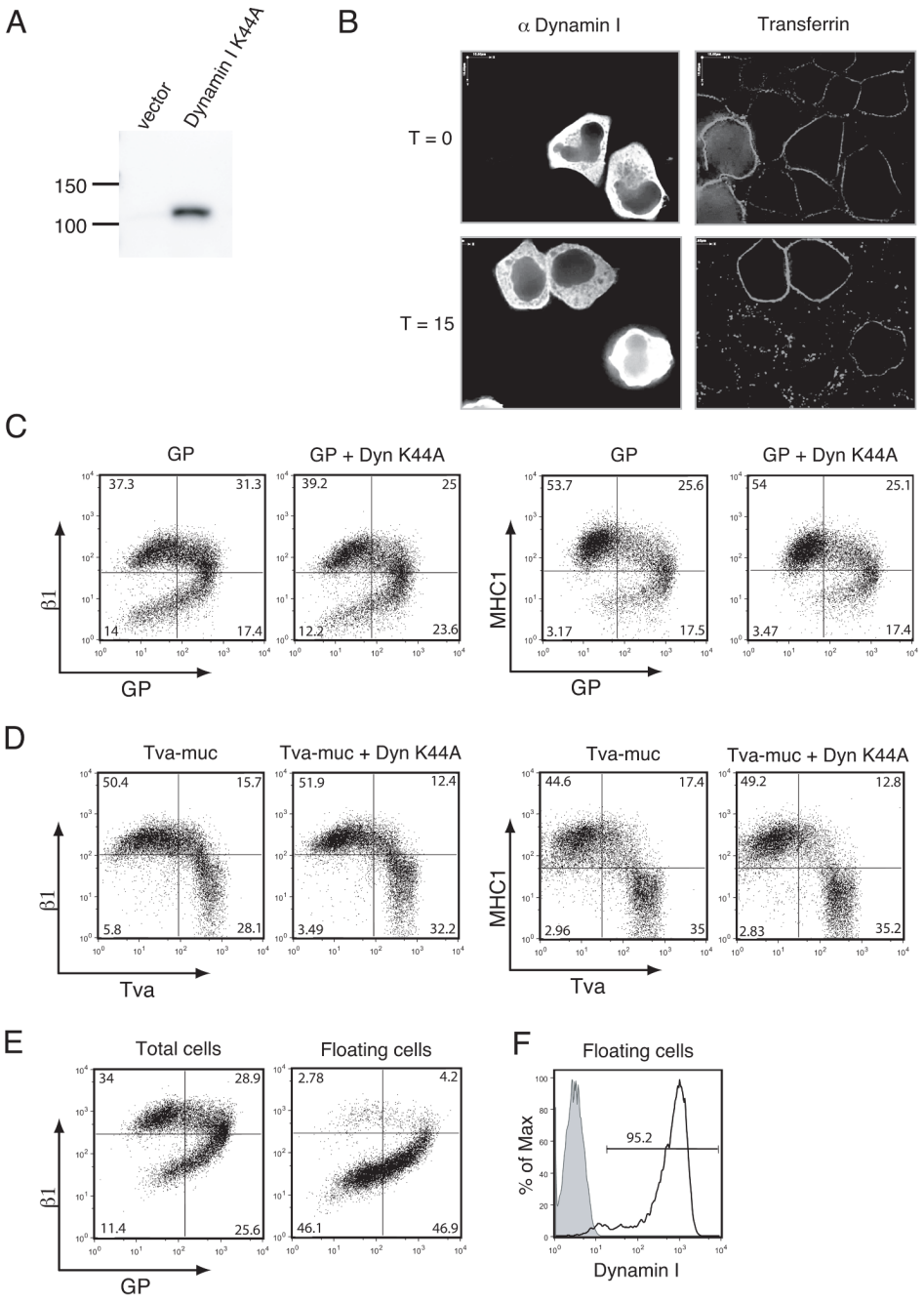

FIG. 5.

GP-mediated surface protein down-regulation is not mediated by dynamin I. (A) 293T cells were transfected with vector alone or vector encoding dynamin I K44A (Dyn K44A). Lysates were harvested in RIPA buffer after 24 h and subjected to SDS-4 to 15% PAGE, transferred to PVDF, and immunoblotted with anti-dynamin I mouse MAb. (B) HeLa cells were transfected with Dyn K44A. After 22 hours, cells were serum starved for 2 hours. Cells were then iced and incubated with Alexa 594-conjugated human transferrin. Cells were either immediately fixed (T=0), or incubated at 37°C for 15 minutes (T=15). Cells were fixed, permeabilized, and stained for dynamin I as described in Materials and Methods, then analyzed by fluorescent microscopy. (C, D) 293T cells were co-transfected (in a 1:3 ratio) with GP and

vector or GP and Dyn K44A (C), Tva-muc and vector or Tva-muc and Dyn K44A (D). Floating and adherent cells were harvested 24 h after transfection, pooled, and stained with antibodies to GP using human monoclonal antibodies and antibodies to Tva using a polyclonal rabbit anti-Tva sera followed by FITC-labeled secondary antibodies, co-stained for β1 integrin or MHC1 with PE-Cy5 conjugated monoclonal antibodies, and assayed by flow cytometry. (E) 239T cells were transfected with GP. After 24 hours, floating cells were either pooled with adherent cells (left plot) or separated from adherent cells (right plot) and stained for GP and β1 integrin as described previously. (F) 293T cells were co-transfected with GP and Dyn K44A (black line) in a 1:3 ratio. Floating cells were harvested after 24 hours, permeabilized, and stained for intracellular dynamin I. Shaded peak represents GP + vector-transfected cells stained for dynamin I. Analyses are shown for events in the live cell gate. Data is representative of multiple independent experiments.